Weissel, J., Peirce, J., Taylor, E., Alt, J., et al., 1991
Proceedings of the Ocean Drilling Program, Scientific Results, Vol. 121

27. DIAGENESIS, HEAT FLOW, AND RIFTING AT BROKEN RIDGE, INDIAN OCEAN[1]

Ian L. Gibson[2]

ABSTRACT

The Broken Ridge tilted and truncated sequence of middle Eocene to Turonian calcareous sediments with intercalated basaltic ash layers is characterized by diagenetic alteration. The level at which opal-CT forms from volcanic glass and the opal-CT/quartz boundary shows that this alteration increases in intensity with stratigraphic depth and is not related to depth below the seafloor. Thus, the rocks were altered before they were tilted and truncated. The preservation of the pre-rift alteration history may be a function of the rapid uplift and erosion following the initiation of spreading between Broken Ridge and the Kerguelen Plateau. The geothermal gradient at the time of rifting, deduced from the pattern of silica diagenesis, agrees with results from present-day heat-flow measurements and suggests that there was no large thermal anomaly at Broken Ridge that time.

INTRODUCTION

"Burial diagenesis" is perhaps the best term for the process that can lead to the formation of zeolites and other secondary minerals, as sediments are successively buried by overlying layers. In relatively undeformed, thick sedimentary basins, the process results in a series of horizontal zones, characterized at increasing depths by progressively higher temperatures and more dehydrated mineral assemblages. The process is similar, or even the same, as the burial metamorphism of Coombs (1954, 1971). However, the alkali zeolites mordenite, analcime, and clinoptilolite, which are common in the marine environment, were explicitly excluded by Coombs (1971) from the metamorphic regime.

The burial diagenetic zoning in late Cenozoic volcaniclastic sediments of the Green Tuff region of Japan (Utada, 1971; Iijima and Utada, 1972) is particularly instructive. In the Niijata oil field, one can demonstrate not only that the zones are flat-lying, but can also correlate the thickness and mineralogy of the zones with the geothermal gradient: it appears that the diagenetic formation of zeolites is proceeding at the present time.

Ocean Drilling Program (ODP) Sites 752, 753, 754, and 755, positioned on a north-south section along Broken Ridge, provide a unique sample through a continuous, tilted sequence of middle Eocene to Turonian chalks and intercalated volcaniclastic horizons underlying a Miocene truncation surface (see Shipboard Scientific Party, 1989, "Broken Ridge Summary" chapter). This brief note on a preliminary X-ray-diffraction (XRD) study of the secondary minerals found in volcaniclastic layers from this sedimentary section has the following broad, general objectives:

1. To document the nature of any secondary mineral zonation in the 1.2-km sedimentary pile.
2. To determine the attitude of any zones relative to the tilted sedimentary succession and the Miocene truncation surface, and thus the relative age of the zones.
3. To assess the geothermal gradient indicated by the zones. Is there evidence of a thermal anomaly related to the nearby Kerguelen hotspot?

The study was restricted to samples from the volcaniclastic layers, to try to reduce the confounding effects of bulk sediment composition on the secondary mineral assemblages. Such effects are known to be important in controlling the development of zeolites and other secondary minerals during burial diagenesis (see, for example, Houghton et al., 1979). However, notwithstanding this approach to sampling, it is obvious from the stratigraphic summary below and the calcium carbonate data in Table 1 that, generally, samples from the stratigraphically lower parts of the section have a higher volcanogenic content and a lower carbonate content than samples from the upper part of the pile.

STRATIGRAPHIC SUMMARY

The total thickness of this pre-Miocene section exceeds 1.2 km. However, the offset nature of the holes drilled, and the lack of complete overlap, resulted in only 0.7 km of the section being sampled during drilling. Although only units with a significant volcanogenic component were sampled, brief notes on the lithologies penetrated during drilling at each site are described below in stratigraphic order, but with comments restricted to rocks underlying the Miocene unconformity. The geographic positions of the sites relative to the stratigraphy are shown diagrammatically in Figure 1.

Site 753

Subunit 753-II (43.6–62.8 mbsf). Middle Eocene calcareous and foraminifer-bearing nannofossil chalks. These are the youngest pre-Miocene rocks penetrated during drilling at Broken Ridge. Only trace amounts of volcanic material are present.

Site 752

Subunit 752-IIa (113–210 mbsf). Lower Eocene to upper Paleocene nannofossil micritic chalk immediately underlying the Miocene unconformity. Two major ash layers over 5 cm thick and several minor ash layers and individual pumice fragments occur within this unit.

Subunit 752-IIb (210–289 mbsf). Upper Paleocene to middle Paleocene nannofossil calcareous chalk with as much as 40% radiolarians and diatoms, and numerous occurrences of volcanic ash. Chert stringers are common.

Subunit 752-IIc (289–436 mbsf). Middle Paleocene to upper Maestrichtian hard chalk. Ash layers are particularly common between 326 and 422 mbsf: the section immediately above the

[1] Weissel, J., Peirce, J., Taylor, E., Alt, J., et al., 1991. *Proc. ODP, Sci. Results*, 121: College Station, TX (Ocean Drilling Program).

[2] Department of Earth Sciences, University of Waterloo, Waterloo, Ontario N2L 3G1, Canada.

Table 1. Summary of Broken Ridge XRF data.

XRD	Hole	Core, section, interval (cm)	Depth (mbsf)	Stratigraphic depth[a]	Silica phase	Heul./Clin.[b]	Clays[c]	Other	Plagioclase	$CaCO_3$ (%)
	753A	6H-2, 36–37	45.5	45.5	Fresh glass; no X-ray data					
	753A	6H-3, 34–35	46.9	46.9						
	753A	7H-3, 35–36	56.6	56.5						
	753A	7H-5, 107–107	60.3	60.3						
54	752B	7R-4, 100–102	321.6	398.6		x	diffuse → 16.5		x	47.6
53	752B	8R-2, 124–127	327.2	404.2	opal-CT?	x	12.5 → 16.5		x	29.7
50	752B	8R-3, 148–150	328.9	405.9	opal-CT?		none → none			
79	752B	10R-7, 25–28	354.4	431.4			none → none		x	24.2
84	752B	11R-1, 41–44	355.2	432.2		x	12.5 → 16.0		x	4.0
85	752B	11R-2, 78–80	357.1	434.1		x	12.0 → 16.2		x	9.5
51	752B	16R-3, 83–86	406.8	483.8			12.5 → 16.5		x	37.0
8	754A	21H-1, 79–81	167.9	509.9		x	11.8 → 16.2			51.5
*0	754B	23H-1, 70–72	171.8	513.8		x	12.2 → 15.9		x	25.0
19	754B	5R-2, 24–25	153.4	495.4		x	11.5 → 16.5		x	59.6
55	754B	7R-1, 28–30	171.0	513.0			12.3 → 16.2	mordenite		56.9
48	754B	9R-2, 78–80	192.6	534.6	opal-CT?	x	12.7 → 17.0	mordenite	x	59.8
49	754B	9R-2, 132–135	193.1	535.1	opal-CT?		12.8 → 16.9	stilbite	x	35.7
47	754B	9R-5, 69–71	197.0	539.0	opal-CT		12.6 → 17.0	mordenite	x	64.1
45	754B	9R-6, 82–83	198.6	540.6	opal-CT	x	12.9 → 16.9	mordenite		58.9
23	754B	9R-6, 103–105	198.8	540.8	opal-CT		12.8 → 16.2	mordenite	x	9.1
44	754B	9R-6, 107–108	198.9	540.9	opal-CT	x	12.4 → 16.2		x	21.8
46	754B	10R-3, 133–134	204.3	546.3	opal-CT		12.8 → 17.0	stilbite	x	51.5
22	754B	11R-1, 80–81	210.4	552.4	opal-CT	x	12.6 → 16.1		x	14.1
21	754B	12R-CC, 0–2	221.0	563.0	opal-CT	x	diffuse		x	66.6
24	754B	13R-3, 50–54	231.4	573.4	opal-CT		12.8 → 16.7	mordenite	x	22.5
25	754B	13R-4, 106–109	233.4	575.4	opal-CT		12.8 → 16.5	stilbite	x	20.5
18	754B	14R-5, 93–95	245.3	587.3	opal-CT	x	13.5 → 17.7		x	19.5
7	754B	15R-3, 96–98	252.2	594.2		x	12.6 → 15.8			25.9
80	754B	15R-3, 102	252.2	594.2		x	10.0 → 13.6		x	27.1
	754B	15R-5, 25–28	254.4	596.4	opal-CT	x	12.7 → 16.7		x	7.4
87	755A	6R-1, 56–58	72.7	1164.2	opal-CT	mordenite	12.6 → 15.8			20.2
86	755A	7R-2, 72–75	84.0	1175.5	quartz	mordenite	12.6 → 16.0		x	13.1
75	755A	9R-1, 128–131	102.5	1194.0	quartz	stilbite			x	16.6
76	755A	12R-1, 1–4	131.1	1222.6	quartz	mordenite	12.6, 14.6 → 16.0		x	18.7
81	755A	13R-3, 75–78	144.4	1235.9	quartz	mordenite	12.9, 14.0 → 16.0		x	20.7
82	755A	14R-2, 62–65	153.9	1245.4	quartz	x	12.8, 14.7 → 16.5		x	18.8
77	755A	18R-6, 123–125	196.8	1288.3	quartz?	x	12.5, 14.2 → 14.2		x	1.7
78	755A	19R-2, 54			quartz	x	14.1 → 14.5		x	
83	755A	19R-6, 12			quartz?	x	14.0 → 15.2		x	2.7

Note: "x" indicates phase identified as present.
[a] At Site 753, stratigraphic depth = mbsf; at Site 752, stratigraphic depth = mbsf + 77 m; at Site 754, stratigraphic depth = mbsf + 342 m; at Site 755, stratigraphic depth = mbsf + 1091.5 m. These transformations assume that 190 m of the section is missing between Sites 753 and 752, that there is a 20-m overlap between Sites 752 and 754, and that 460 m of the section is missing between Sites 754 and 755.
[b] The zeolites heulandite and clinoptilolite.
[c] Numbers indicate the angstrom spacing of the major basal reflection of air-dried and glycolated samples.

Cretaceous/Tertiary boundary at 358 m is particularly rich in volcanic material.

Site 754

Subunit 754-IIa (151–190 mbsf). Upper Maestrichtian chalk with planar and cross-bedded laminae. The chalk is mottled in places with chert and pyrite filling burrows. Ash layers occur regularly, many containing from 10% to 50% ash. Chert layers several centimeters thick also occur.

Subunit 754-IIb (190–287 mbsf). Laminated Maestrichtian limestone. Ash layers with ash contents up to 75% are common, and darken the host sediment. Several chert layers occur between 258 and 268 mbsf.

Subunit 754-IIc (287–355 mbsf). Poorly recovered lower Maestrichtian limestone and chert sequence with some intercalated ash layers.

Site 755

Subunit 755-IIa (65.5–140.8 mbsf). Lower Santonian to lower Coniacian/upper Turonian tuff with interbedded ashy limestone. The subunit contains from 50%–90% ash with the proportion of micrite decreasing downsection. Thin porcellanite layers with chert fragments occur sporadically.

Subunit 755-IIb (140.8–189 mbsf). Lower Coniacian/upper Turonian to lower Turonian tuffs with glauconite which decreases in abundance downsection. The unit, which contains from 40%–80% ash, is moderately bioturbated and mottled.

Subunit 755-IIc (189–208.4 mbsf). Turonian tuffs (60%–90% ash) with some micrite and glauconite-rich layers in the upper 10 m of this subunit.

The most obvious feature of this pre-Miocene section is the downward increase in the proportion of volcanic material in the section and the increasingly indurated nature of the rocks.

EXPERIMENTAL PROCEDURES

Ash-rich horizons were sampled during routine shipboard core description, primarily for X-ray-fluorescence (XRF) analysis, to determine the bulk trace-element composition of the sediment samples, and hence the general character of the igneous component. The results of this work are presented in the Leg 121 *Initial Reports* (Shipboard Scientific Party, 1989, "Broken Ridge Summary" chapter), along with the calcium carbonate concentrations of the studied samples.

The same material was also used for an X-ray-diffraction study of the mineral phases present in the volcaniclastic units, using the shipboard Phillips ADP 3520 X-ray diffractometer for the analy-

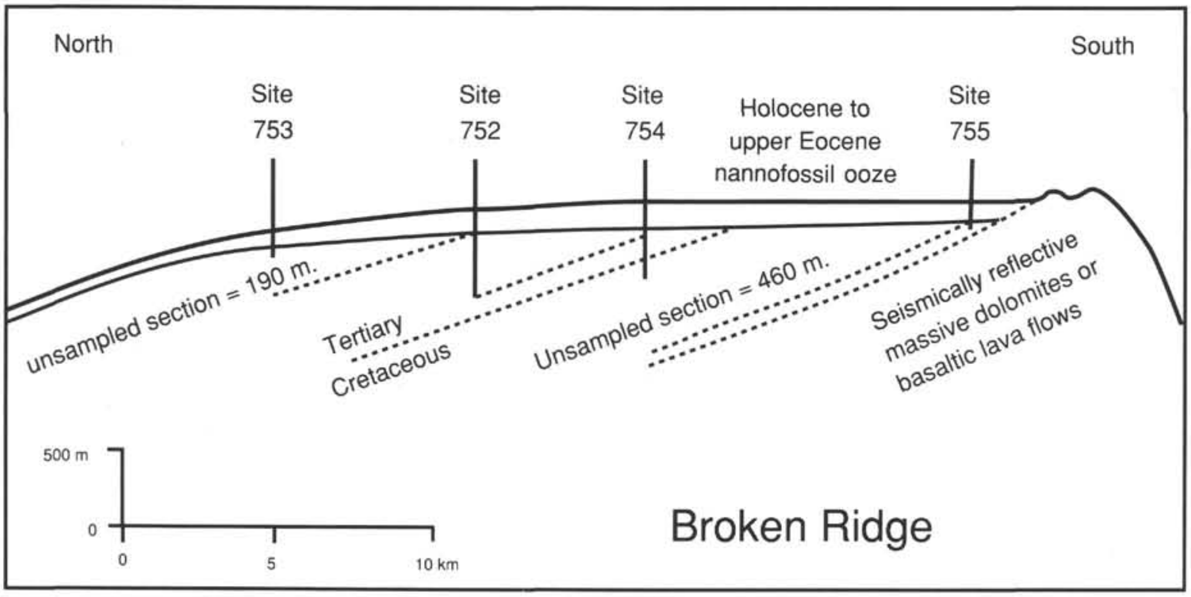

Figure 1. Diagrammatic section through Broken Ridge showing the location of the Leg 121 sites which penetrate the middle Eocene to Turonian succession.

sis. The instrumental conditions used were CuKα radiation with a Ni filter, operating power 40 Kv and 35 mA, goniometer scan from 2° to 30° 2θ, step-size 0.02°, and 1-s count-time per step. Samples were scanned twice: once after air-drying and secondly after treatment with ethylene glycol. No heating experiments were carried out, limiting the interpretation of the clay mineral and zeolite data.

Very little onboard interpretation of the resulting diffractograms was completed and most of this work has been completed subsequently using the standard powder diffraction files and the tabulated data for clay minerals of Brindley and Brown (1980).

RESULTS

The X-ray-diffraction results are presented in Table 1. These clearly show that the alteration assemblage changes and becomes more diverse with stratigraphic depth. This has been emphasized in Table 1 by the listing of the results in stratigraphic order, and by including in the table an approximate calculated stratigraphic depth for each sample. The basis for this calculation is shown in the notes to Table 1. As noted above, there is also a generally downward progressive increase in the proportion of ash in the sedimentary section as indicated by a decrease in the proportion of calcium carbonate with depth (see table 1 and fig. 9 in Shipboard Scientific Party, 1989, "Broken Ridge Summary" chapter). At the stratigraphically lower Broken Ridge sites, the included volcanic glass is altered, releasing silica and leading to the formation of a variety of diagenetic minerals including clay minerals, zeolites, and the silica phases of opal-CT and quartz.

Changes in the clay minerals are marked only in the lower part of the section. At Sites 752 and 754 mixed-layered smectite-chlorites are dominant. However, in a few samples from the lower part of Hole 755A, chlorite, characterized by a 14A basal reflection after treatment with ethylene glycol, is the dominant clay mineral, indicating a change to a higher pressure/temperature phase. This change in the clay mineralogy to chlorite has been recognized in other marine sequences developed during burial diagenesis (Iijima, 1978).

The diagenetic zeolite assemblage is dominated by the occurrence of what is tentatively identified as a Ca-rich clinoptilolite at Site 752 and is associated with a Ca-rich mordenite below a stratigraphic depth of about 500 m in the section at Sites 754 and 755. Kastner (1980) noted that, in the absence of heating experiments, the X-ray-diffraction distinction between clinoptilolite and heulandite is very difficult, but the latter phase probably dominates in the lower part of the stratigraphic section (see notes for Table 1).

The silica phases, opal-CT and quartz, also show vertical changes with stratigraphic depth. The uppermost part of the section, drilled at Site 753, shows minimal effects of alteration, and fresh glass is present. Siliceous diatoms are also well preserved at this site but absent at stratigraphically lower levels of the pre-Miocene section at Sites 754 and 755 (Shipboard Scientific Party, 1989). At these lower sites the volcanic glass is generally altered, and at Site 754, below the Tertiary/Cretaceous boundary, fresh glass is absent. The alteration appears to involve the formation of clay minerals and zeolites and the formation of opal-CT, which can be identified in most of the samples from the lower part of Hole 754B (Table 1). The opal-CT/quartz transition falls in the unsampled interval between the bottom of Hole 754B and Hole 755A, at a stratigraphic depth of between 800 and 900 m, and diagenetic quartz is developed in almost all of the studied samples in Hole 755A.

DISCUSSION

Silica Mineralogy and Observed Physical Properties

The most significant change in the physical properties noted in the Leg 121 *Initial Reports* (Shipboard Scientific Party, 1989, "Broken Ridge Summary" chapter, fig. 40) is the marked increase in the density of the calcareous sediments, from an overall bulk density of less than 2.0 g/cm^3 to a density of about 2.25 g/cm^3. This change takes place progressively at a stratigraphic depth between 450 and 550 m. The change is also associated with an increase in sonic velocities and a lithologic change from chalks to limestones. Siliceous diatoms are also poorly preserved or absent below this transition, and chert becomes an important element in the lithostratigraphy.

The data presented in Table 1 suggest that this density change appears to correspond with the appearance of opal-CT and probably with the opal-A/opal-CT transition. However, the change is not simply the result of the formation of a denser form of SiO_2; the destruction of siliceous diatoms and increased compaction are probably more important contributing factors. The mineralogical transition is not abrupt, probably because the bulk silica content of the sediments is very variable, depending on the basaltic ash content. Opal-CT has been identified in more that half of the samples from Hole 754B.

The opal-CT/quartz transition, which falls in the unsampled interval between the bottom of Hole 754B and Hole 755A, at a stratigraphic depth of between 800 and 900 m, does not appear to be marked by further changes in the physical properties. There is again only a relatively small change in the density of the silica phases, and this diagenetic change may be masked by changes in the nature of the sediments; the rocks from the lower part of Hole 755A are particularly rich in basaltic material and its alteration productions.

Iijima (1978) described the transition from mixed-layered smectite-chlorites to chlorite as occurring below the level of the opal-CT/quartz transition in a series of silica-saturated sediments from northern Japan. The same relative position of the two boundaries is observed at Broken Ridge. Mordenite also appears in the two sections at about the same stratigraphic level. These parallel changes in the silica, zeolite, and clay mineralogy in the two areas is important because it suggests that in general: (1) the silica minerals, zeolites, and clays form a quasi-equilibrium assemblage and (2) the positions of the diagenetic alteration zones are being controlled by the pressure/temperature conditions, as the bulk composition of the sediments in the two areas is rather different. In general, in deep-sea sediments, opal-CT is more common in clay-rich sediments and quartz is more common in carbonate sediments (see, for example, Lancelot, 1973; Kastner et al., 1977). This also suggests that the opal-CT/quartz boundary at Broken Ridge is not a function of changing bulk-sediment compositions, as clays are more abundant in the deeper, quartz-bearing section in Hole 755A.

Calculated Geothermal Gradient

The observed secondary minerals at Broken Ridge are clearly samples from disequilibrium assemblages: the higher temperature rocks containing diagenetic quartz from Hole 755A are from some of the shallowest sections. If it is assumed that the uplift, tilting, and erosion of the tilted sequence of middle Eocene to Turonian sediments was a rapid geological process, and that the retrogression of the quartz-bearing assemblages was slow, the observed diagenetic mineral assemblages should reflect the pre-tilting geothermal environment and can be used to calculate the former geothermal gradient.

The transformation of siliceous phases, from opal-A through opal-CT to quartz, with increasing depth and temperature is widely recognized but perhaps best documented in the Neogene diatomaceous siliceous sediments of northern Japan (Iijima and Tada, 1981). These workers demonstrated from bottom-hole temperature measurements that the opal-A/opal-CT conversion starts at between 22°–23°C, and that the opal-CT/quartz transition is complete at about 72°C. Shipboard scientists on Leg 127 made downhole temperature measurements at Sites 794, 795, and 797 in the Japan Sea and showed that the temperature for opal-A/opal-CT conversion and the associated change in the physical properties averaged 40°C.

The transition from opal-A to opal-CT was estimated to occur at Broken Ridge at a stratigraphic depth of 500 m. Using the paleotemperature estimate of 40°C and a sea-bottom temperature of 2°C, this translates into a temperature gradient of 76°C/km.

The transition from opal-CT to quartz was estimated to occur at Broken Ridge at a stratigraphic depth of 800–900 m. Using the temperature estimates from northern Japan noted above, this reflects a fossil temperature gradient of about 80°C/km.

These two temperature gradients and the observed thermal conductivities of the cores (1.5 W/m · K) suggest that the heat flow at the time of uplift and erosion of Broken Ridge was about 120 mW/m^2.

In Figure 2, this new heat-flow determination is superimposed on the data from the *Initial Reports* (Shipboard Scientific Party, 1989, "Broken Ridge Summary" chapter, fig. 42). Three reliable heat-flow determinations were made at Sites 752 and 753 during Leg 121. The present-day heat flow calculated from these three values averages 44.8 mW/m^2 and the new determination lies above the model line of Anderson et al. (1977). Although there is considerable uncertainty associated with the calculation of the "fossil" heat flow, the results in general substantiate the preliminary conclusion that there was no significant thermal event at Broken Ridge during the middle Eocene.

Alteration and Deformation at Broken Ridge

The work on the secondary mineralization reported here suggests that the major features of the diagenesis of the pre-rift sedimentary succession were established prior to the rifting event and that only minor changes have taken place during the subsequent 40 Ma. This may be because the rifting event that resulted in the uplift and tilting of Broken Ridge was brief, perhaps lasting less than 5 m.y., the event suddenly curtailing and stabilizing the earlier diagenetic regime (Shipboard Scientific Party, 1989, "Broken Ridge Summary" chapter).

CONCLUSIONS

1. The tilted sequence of middle Eocene to Turonian sediments at Broken Ridge is characterized by diagenetic alteration which

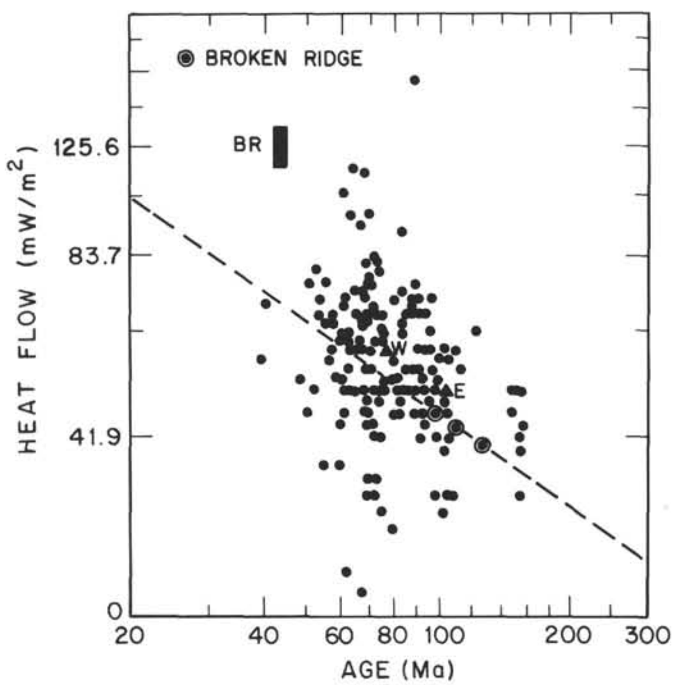

Figure 2. Graph of heat flow vs. age for the Indian Ocean crust older than 40 Ma. Results from Leg 121 and Anderson et al. (1977) at Broken Ridge are plotted on the modeled relationship for this crust. Modified from the Leg 121 *Initial Reports* (Shipboard Scientific Party, 1989, "Broken Ridge Summary" chapter, fig. 42). Abbreviations: BR = calculated heat flow at Broken Ridge at 42 Ma.

increases in intensity with stratigraphic depth and is not related to the depth below seafloor.

2. The preservation of the pre-rift alteration history may be a function of the rapid uplift and erosion following the initiation of spreading between Broken Ridge and the Kerguelen Plateau.

3. The geothermal gradient at the time of rifting, deduced from the pattern of silica diagenesis (about 120 mW/m^2), supports the present-day heat-flow measurement, which suggests that there was no large thermal anomaly at Broken Ridge at that time.

REFERENCES

Anderson, R. N., Langseth, M. G., and Sclater, J. G., 1977. The mechanism of heat transfer through the floor of the Indian Ocean. *J. Geophys. Res.*, 82:3391–3409.

Brindley, G. W., and Brown, G. (Eds.), 1980. *Crystal Structures of Clay Minerals and Their X-ray Identification*. Mineral. Soc. Monogr., 5.

Coombs, D. S., 1954. The nature and alteration of some Triassic sediments from Southland, New Zealand. *Trans. R. Soc. N. Z.*, 82:65–109.

_______, 1971. Present status of the zeolite facies: Molecular Seive Zeolites—1. *Adv. Chem. Ser.*, 101:317–327.

Houghton, R. L., Rothe, P., and Galehouse, J. S., 1979. Distribution and chemistry of phillipsite, clinoptilolite, and associated zeolites at DSDP sites 382, 385, and 386 in the western North Atlantic. *In* Tucholke, B. E., Vogt, P. R., et al., *Init. Repts. DSDP*, 43: Washington (U.S. Govt. Printing Office), 463–483.

Iijima, A., 1978. Geological occurrences of zeolite in marine environments. *In* San, L. B., and Mumpton, F. A., (Eds.), *Natural Zeolites Occurrence, Properties, Use:* Oxford (Pergamon Press), 175–198.

Iijima, A., and Tada, R., 1981. Silica diagenesis of Neogene diatomaceous and volcaniclastic sediments in northern Japan. *Sedimentology*, 28:185–200.

Iijima, A., and Utada, M., 1972. A critical review on the occurrence of zeolites in sedimentary rocks in Japan. *Jpn. J. Geol. Geogr.*, 42: 342–349.

Kastner, M., 1980. Silica polymorphs. *In* Burns, R. G. (Ed.), *Marine Minerals*. Min. Soc. Am. Rev. Mineral., 6:99–109.

Kastner, M., Keene, J. B., and Gieskes, J. M., 1977. Diagenesis of siliceous oozes. I. Chemical controls on the rate of opal-A to opal-CT transformation—an experimental study. *Geochim. Cosmochim. Acta*, 41:1041–1059.

Lancelot, Y., 1973. Chert and silica diagenesis in sediments from the central Pacific. *In* Winterer, E. L., Ewing, J. I., et al., *Init. Repts. DSDP*, 17: Washington (U.S. Govt. Printing Office), 377–405.

Shipboard Scientific Party, 1989. Broken Ridge summary. *In* Peirce, J., Weissel, J., et al., *Proc. ODP, Init. Repts.*, 121: College Station, TX (Ocean Drilling Program), 457–506.

Utada, M., 1971. Zeolitic zoning in the Neogene pyroclastic rocks of Japan. *Sci. Papers Coll. Gen. Educ. Univ. Tokyo*, 21:189–221.

Date of initial receipt: 1 May 1990
Date of acceptance: 12 November 1990
Ms 121B-164